

**REGOLITH CHARACTERISTICS OF THE REINER GAMMA SWIRL AS REVEALED BY POLARIMETRIC OBSERVATIONS.** M. Bhatt<sup>1</sup>, C. Wöhler<sup>2</sup>, Aravind K.<sup>1,3</sup>, S. Ganesh<sup>1</sup>, A. Bhardwaj<sup>1</sup>. <sup>1</sup>Physical Research Laboratory, Ahmedabad, 380009, India. <sup>2</sup>Image Analysis Group, TU Dortmund University, Otto-Hahn-Str. 4, 44227 Dortmund, Germany. <sup>3</sup>Indian Institute of Technology, Gandhinagar, 382355, India (megha@prl.res.in).

**Introduction:** Lunar swirls are high-albedo curvilinear markings always associated with magnetic anomaly regions but not associated with distinct topography [1, 2]. Among all known swirls on the Moon, Reiner Gamma is a specific case with a fully evolved structure of high-albedo curve-shaped line markings extended across an area of about 200 km<sup>2</sup>. The recent spectral observations of Reiner Gamma suggest low surface hydration on swirls indicating reduced space weathering due to magnetic shielding (e.g., [2,3,4]). However, the variation in spectral properties found at swirl locations in the near infrared wavelength domain cannot always be explained by reduced space-weathering alone [4, 5].

In this work we aim to understand the structure of Reiner Gamma regolith using ground based polarimetric observations. We adopted a comparative approach and thus also observed the craters Kepler Aristarchus with the prominent ray systems.

**Observations and analysis:** The polarimetric observation data sets were obtained at the Mount Abu IR Observatory on 5<sup>th</sup> and 6<sup>th</sup> January, 2021 using the electron multiplying CCD based optical imaging polarimeter (EMPOL) developed in-house [6]. The observations were collected with two narrow band continuum filters GC (green) and RC (red) [7]. The number of steps per rotation is 48. Here we present results obtained using GC filter observations at phase angles of 84° and 98°. The data were corrected using appropriate dark frames and flatfield frames.

We derived total intensity  $I$ , Amplitude  $A$ , the linear polarization fraction  $P$ , and the angle of the orientation  $W$  from the acquired 48-image sets. Furthermore, we derived the phase ratio maps by dividing mean intensity images at 98° by those at 84°.

**Results and Discussion:** Polarimetric data of the lunar surface provide information on regolith characteristics such as grain size and roughness [8]. We compare the polarization parameters derived for the Reiner Gamma swirl with the regions around the craters Kepler and Aristarchus as shown in Fig. 1, while Fig. 2 shows the phase ratio images.

A “normal” polarization behavior is described by the Umov law stating that the polarization fraction is inversely proportional to the albedo [9]. This implies that the amplitude  $A$  is constant when the Umov law is valid. As the polarization fraction increases with increasing grain size [8], positive anomalies of  $A$

correspond to a larger grain size and negative anomalies to a smaller grain size, compared to the surrounding surface.

The slope of the phase angle dependent reflectance function increases with increasing surface roughness [10]. Hence, in our phase ratio images small ratios correspond to a steep slope of the reflectance function (implying a rough surface) and large ratios to a low slope (implying a smooth surface). The forward vs. backward scattering behavior of the regolith grains described by the single-particle scattering function also has an influence on the slope of the reflectance function [10], but this influence is likely to be weak at phase angles around 90° “between” the scattering lobes.

Accordingly, our data suggest that the surface of the main oval of Reiner Gamma is more finely grained (negative anomaly in  $A$ ) and smoother (positive anomaly in phase ratio) than the surrounding mare surface. The surface of the small swirl patterns southwest of the main oval has similar properties as the surface of the main oval. The surface of the northeastern “tail” is similarly finely grained as the main oval (similarly strong anomaly in  $A$ ) but smoother (stronger positive phase ratio anomaly). These anomalies in the tail correlate with the soil compaction found spectrally in [4]. The surface of the area immediately southeast of the main oval has coarser grains (positive anomaly in  $A$ ) and a rougher surface (negative phase ratio anomaly) than the main oval and the surrounding mare surface. This area is also visible in the phase ratio images of [11]. The ray systems of Aristarchus and Kepler do not show anomalies in the  $A$  image and the phase ratio image. Hence, their grain size and roughness values do not differ significantly from the surrounding mare surface.

The complete Reiner Gamma swirl, including the northeastern tail and the southwestern patterns, exhibits a positive anomaly in polarization angle, whereas the area immediately southeast of the main oval shows a negative anomaly. It is not clear which surface properties (apart from topographic structures, which are absent for Reiner Gamma) may lead to such angle anomalies. The ray systems of Aristarchus and Kepler do not show angle anomalies in our data.

The phase ratio anomalies of Reiner Gamma partially correlate with the spectrally derived soil compaction areas of Reiner Gamma derived in [4].

**Summary:** Based on telescopic polarimetric analysis, we found that the regolith properties of Reiner Gamma are different from those of its surroundings and the examined crater ray systems. The anomalies observed in the polarization parameter and phase ratio maps suggest the occurrence of surface alteration processes that might have disrupted the regolith microstructure on the swirl. These findings are consistent with an external mechanism of swirl formation by interaction between the regolith and cometary gas [4, 12, 13].

**Acknowledgments:** We acknowledge Mount Abu observatory staff for technical help. Work at PRL is funded by the Dept. of Space, Govt. of India.

**References:** [1] Hood L. et al. (1979) *Science* 204, 53-57. [2] Blewett, D. T. et al. (2011) *JGR* 116, E02002. [3] Wöhler, C. et al. (2017) *Sci. Adv.* 3, e1701286. [4] Hess M. et al. (2020) *A&A* 639, A12. [5] Bhatt M. et al. (2018) *LPSC XLIX*, abstract 1765. [6] Ganesh S. et al. (2020) *Proc. SPIE* 11447, Ground-based and Airborne Instrumentation for Astronomy VIII, 114479E. [7] Farnham T. L. et al. (2000), *Icarus* 147, 180-204. [8] Dollfus A. (1999), *Icarus* 140, 313-327. [9] Shkuratov et al. (2011) *PSS* 59(13), 1326-1371. [10] Hapke, B. (2012) *Theory of Reflectance and Emittance Spectroscopy*, 2<sup>nd</sup> ed., Cambridge Univ. Press. [11] Opanasenko, N. and Shkuratov, Y. (2004) *LPSC XXXV*, abstract 1493. [12] Schultz, P. H. and Srnka, L. J. (1980) *Nature* 284, 22-26. [13] Shevchenko, V. V. (1993) *Astron. Rep.* 37, 314-319.

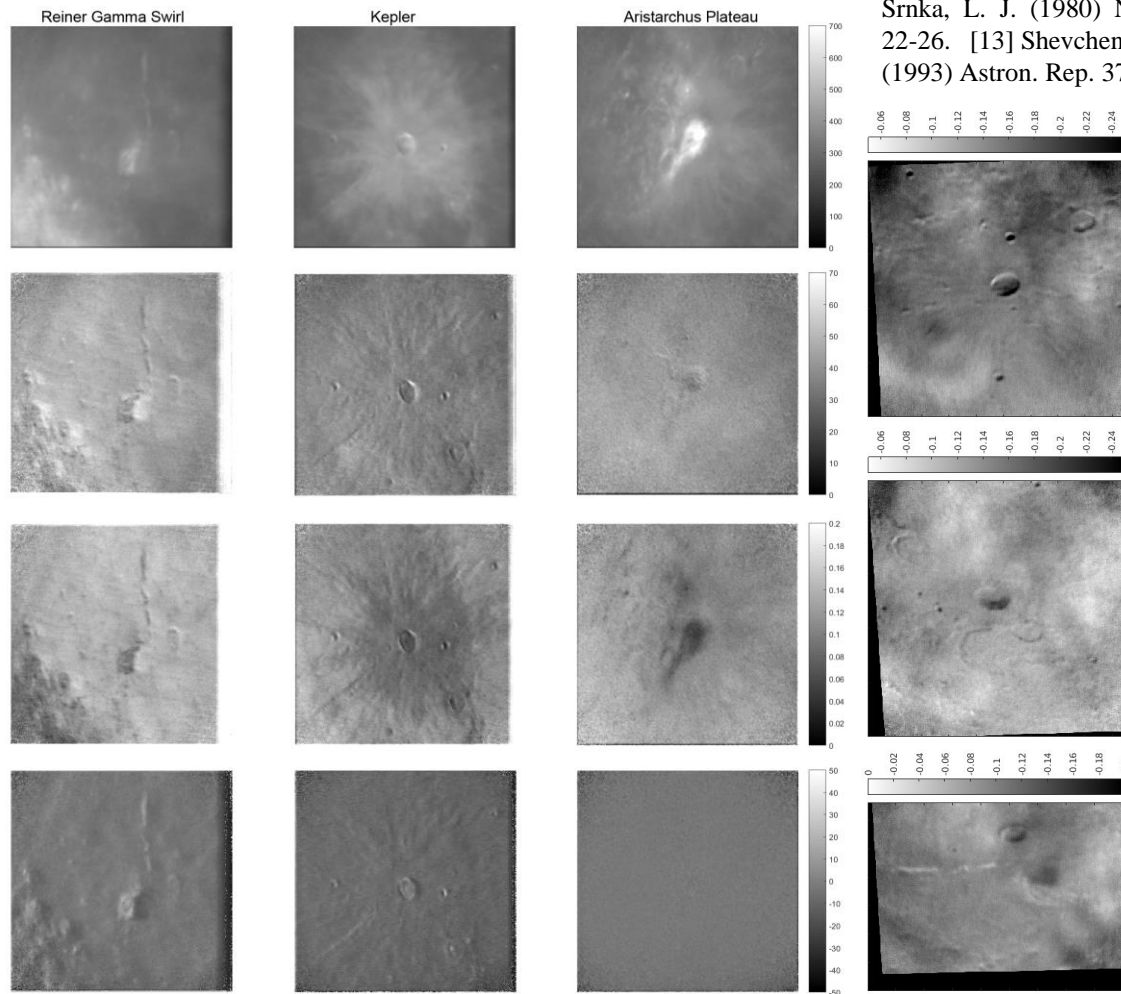


**Fig. 1:** A comparison of polarization parameters derived from our telescopic observations of the Reiner Gamma swirl and the craters Kepler and Aristarchus. The rows show (from top to bottom) the total intensity (in DN), the amplitude (in DN), the polarization fraction and the angle of orientation (in degrees), respectively.

**Fig.2:** Phase ratio ( $98^\circ/84^\circ$ ) maps of Reiner Gamma (left), Kepler (center) and Aristarchus (right). The ratio is shown in logarithmic scale for better visibility of structures.